(*Special Issue on Microwave Filters*), vol. MTT-13, pp. 676–692, Sept. 1965.
[10] H. E. Stinehelfer, Sr., "An accurate calculation of uniform microstrip transmission lines," *IEEE Trans. Microwave Theory Tech.* (*Special Issue on Microwave Integrated Circuits*), vol. MTT-16, pp. 439–444, July 1968.
[11] M. A. Earle and P. Benedek, "Characteristic impedance of dielectric supported strip transmission line," *IEEE Trans. Microwave Theory Tech.* (Corresp.), vol. MTT-16, pp. 884–885, Oct. 1968.
[12] W. T. Weeks, "Calculation of coefficients of capacitance of multiconductor transmission lines in the presence of a dielectric interface," *IEEE Trans. Microwave Theory Tech.*, vol. MTT-18, pp. 35–43, Jan. 1970.
[13] T. G. Bryant and J. A. Weiss, "Parameters of microstrip transmission lines and of coupled pairs of microstrip lines," *IEEE Trans. Microwave Theory Tech.* (*1968 Symp. Issue*), vol. MTT-16, pp. 1021–1027, Dec. 1968.
[14] E. Yamashita and K. Atsuki, "Analysis of thick-strip transmission lines," *IEEE Trans. Microwave Theory Tech.* (Corresp.), vol. MTT-19, pp. 120–122, Jan. 1971.
[15] E. Costamagna, "Fast parameters calculation of the dielectric-supported air-strip transmission line," *IEEE Trans. Microwave Theory Tech.* (Lett.), vol. MTT-21, pp. 155–156, Mar. 1973.
[16] A. Farrar and A. T. Adams, "A potential theory method for covered microstrip," *IEEE Trans. Microwave Theory Tech.* (Short Papers), vol. MTT-21, pp. 494–496, July 1973.
[17] P. Silvester, "TEM wave properties of microstrip transmission lines," *Proc. Inst. Elec. Eng.*, vol. 115, pp. 43–48, Jan. 1968.
[18] A. Farrar and A. T. Adams, "Characteristic impedance of microstrip by the method of moments," *IEEE Trans. Microwave Theory Tech.* (Corresp.), vol. MTT-18, pp. 65–66, Jan. 1970.
[19] B. L. Lennartsson, "A network analogue method for computing the TEM characteristics of planar transmission lines," *IEEE Trans. Microwave Theory Tech.*, vol. MTT-20, pp. 586–591, Sept. 1972.
[20] N. Levinson, *The Wiener RMS (Root Mean Square) Error Criterion in Filter Design and Prediction.* Cambridge, Mass.: M.I.T. Press, 1964 (appendix: time series by N. Wiener), pp. 130–148.
[21] R. T. Gregory and D. L. Karney, *A Collection of Matrices for Testing Computational Algorithms.* New York: Wiley, 1969, pp. 134–142.
[22] H. Sobol, "Extending IC technology to microwave equipments," *Microwaves*, Mar. 20, 1967.

Calculation of Microstrip Discontinuity Inductances

ALISTAIR F. THOMSON AND ANAND GOPINATH, MEMBER, IEEE

Abstract—**Inductive components of microstrip discontinuity equivalent circuits are calculated by the Galerkin method. The formulation and method of calculation are discussed and a large number of numerical results for symmetric corners, T junctions, and steps changes are presented. These results compare well with experiment.**

INTRODUCTION

THE characterization of microstrip discontinuities by equivalent circuits is currently of some interest. Detailed knowledge of the parameters in these circuits enables easy implementation of paper designs without tedious cut-and-try methods. While the published literature [1]–[4] provides curves for the capacitive components of these circuits, little is available for their inductive components. The method of calculation suggested by Horton [5], [6] is not rigorous since the inductance calculation is based on charge estimates and the results obtained are not in agreement with experiment. The magnetic wall model has been used for triplate lines which are wide and homogenous and have confined fields, but its extension to microstrip lines which are inhomogenous and much narrower in comparison and are open structures is not completely justified.

Quasi-static calculation of inductance by the moment method [7] has provided results which show reasonable agreement with experiment. However, the disadvantage of this method for these three-dimensional problems as shown by Farrar and Adams [1] is the very large computer store requirements even for modest discretization. The alternative is to use a finite-element method as in the skin-effect formulation [8]. The results of discontinuity inductance from this method obtained previously were inaccurate as they were arrived at by subtracting two nearly equal numbers. Also the method was limited to finite-length strips and thus could not represent the actual situation in which the strips extend so far from the discontinuity that they may be considered as semi-infinite. The present paper is an extension of this finite-element method which overcomes these difficulties, and the results obtained for right-angled bends, step-width changes, and symmetrical T junctions are presented in the form of curves. Comparison of the results with experiment [9] shows reasonable

Manuscript received November 19, 1974; revised March 27, 1975. The work of A. F. Thomson was supported by a Science Research Council Studentship.

The authors are with the School of Electronic and Engineering Science, University College of North Wales, Bangor, Caerns., LL57, 1UT, Wales, U. K.

agreement with extrapolated low-frequency values, valid up to 5 GHz with 0.020-in alumina substrate. Unfortunately, these inductive components are frequency dependent, and quasi-static calculation can provide only their low-frequency values. However, in the absence of any rigorous time-dependent solution, it is hoped that the method and associated results given here provide a firm starting point for designers.

The computer program developed for this work is capable of providing data on a variety of discontinuities provided that these have Manhattan-type geometries. This limitation is due to a singularity in the Green's function which is easily integrable only over a rectangular element. However, this limitation may be circumvented at the expense of computation time, but was not considered worthwhile at the present time.

The data presented in this paper could be obtained experimentally as demonstrated by Easter [9]. But the experiments need to be carefully performed and the evaluation of the equivalent circuit of one example of the symmetric T requires a large number of measurements. Since such experimental data is never comprehensive, the calculation outlined here provides a low-frequency value of the inductive components for a variety of discontinuity geometries.

FORMULATION OF PROBLEM

The formulation assumes quasi-static conditions which imply the following: the size of the discontinuity is small compared to the wavelength; retardation effects can be neglected; the current on the strip has zero divergence.

Since inductive calculations are involved, the presence of the dielectric substrate (provided it is nonmagnetic) may be disregarded, and only the discontinuity structure and its image in the ground plane need be considered. The discontinuity is assumed to be the junction of two or more semi-infinite uniform lines.

The magnetic vector potential $\bar{A}$ due to the current density $\bar{J}$ on any section of the line or discontinuity is given by

$$\bar{A} = \mu_0 \int G\bar{J}\, dV \tag{1}$$

where the Green's function G is

$$G = \frac{1}{4\pi[(x - x_0)^2 + (y - y_0)^2 + (z - z_0)^2]^{1/2}}.$$

From Maxwell's equations, the electric field in the discontinuity structure is

$$\bar{E} = -\frac{\partial \bar{A}}{\partial t} - \nabla\phi \tag{2}$$

where ϕ is the scalar impressed potential. Ohm's law requires that

$$\bar{J} = \sigma\bar{E} \tag{3}$$

where σ is the conductivity of the strip structure. Substituting from (1) and (3) into (2) gives

$$\bar{J} + \mu_0\sigma \frac{\partial}{\partial t} \int G\bar{J}\, dV = -\sigma\nabla\phi \tag{4}$$

which is the integro-differential skin-effect equation. Since we are only concerned with microstrip lines where σ is very large and the frequency of operation is high, the first term in (4) is small and may be neglected to give

$$\mu_0\sigma \frac{\partial}{\partial t} \int G\bar{J}\, dv \approx -\nabla\phi. \tag{5}$$

This is equivalent to saying that the impressed electric field in the strip conductor is balanced by the magnetically induced fields, and the ohmic drop is negligible.

The curl of (5) gives

$$\nabla \times \mu_0 \frac{\partial}{\partial t} \int G\bar{J}\, dV = \frac{\partial \bar{B}}{\partial t} = 0 \tag{6}$$

which is the high-frequency condition when zero flux penetrates the conductors.

The divergence of (5) gives

$$\nabla^2\phi = 0 \tag{7}$$

i.e., the impressed potential satisfied Laplace's equations on the strip conductors.

Thus the governing equations to be solved for this problem are (5) and (7) or, alternatively, (6). The former two equations were solved as it is inconvenient in this finite-element implementation to use (6) because the integration of the associated Green's function in (6) is computationally lengthy. The solutions of (7) for ϕ, and then (5) for the current density $\bar{J}$ enable the inductance of the stripline structure to be obtained from the following relationships:

$$\int \bar{A}\cdot\bar{J}\, dV = I^2L \tag{8}$$

and

$$\int \bar{J}\, dS = I. \tag{9}$$

METHOD OF SOLUTION

For convenience, the strip is assumed to be thin, and therefore the current density $\bar{J}$ is uniform across the thickness of the strip τ. Thus $\bar{J}$ is a two-dimensional vector, and volume integrals become surface integrals and surface ones become line integrals. Equation (5) thus becomes

$$j\omega\mu_0\tau \int G_i\bar{J}\, dS = -\nabla\phi \tag{10}$$

where

- τ thickness of the strip conductor;
- ω angular frequency;
- G_i modified Green's function which includes the ground

plane images

$$G_i = \frac{1}{4\pi[(x - x_0)^2 + (y - y_0)^2]^{1/2}} - \frac{1}{4\pi[(x - x_0)^2 + (y - y_0)^2 + (2h)^2]^{1/2}}$$

h thickness of the substrate.

Define a new variable Φ

$$\Phi = \phi/(j\omega\tau)$$

and (10) becomes

$$\mu_0 \int G_i \bar{J}\, dS = -\nabla\Phi \tag{11}$$

and furthermore, (7) becomes

$$\nabla^2\Phi = 0. \tag{12}$$

The problem requires to be solved over the whole discontinuity structure including the semi-infinite lines, and this becomes impractical without further modifications. However, the effects of the discontinuity fields diminish rapidly from the junction as can be seen by solving Laplace's equation in each case by conformal transformation and noting how far from the discontinuity $\nabla\Phi$ is perturbed from the uniform field condition. Thus at some distance the current distributions and inductances of the lines can be assumed to be that of equivalent infinite uniform lines. Reference planes are defined at these positions and for a right-angled symmetrical bend discontinuity; these are PP' and QQ' as shown in Fig. 1, distance l from the discontinuity reference planes MM' and NN'. The equation need only be solved in the strip region bounded by the planes PP' and QQ', with the constraint that the solution matches that of the inifinite uniform strip solution at these bounding planes. The magnetic vector potential due to the semi-infinite lines terminating at these planes PP' and QQ' also requires to be taken into consideration in (11).

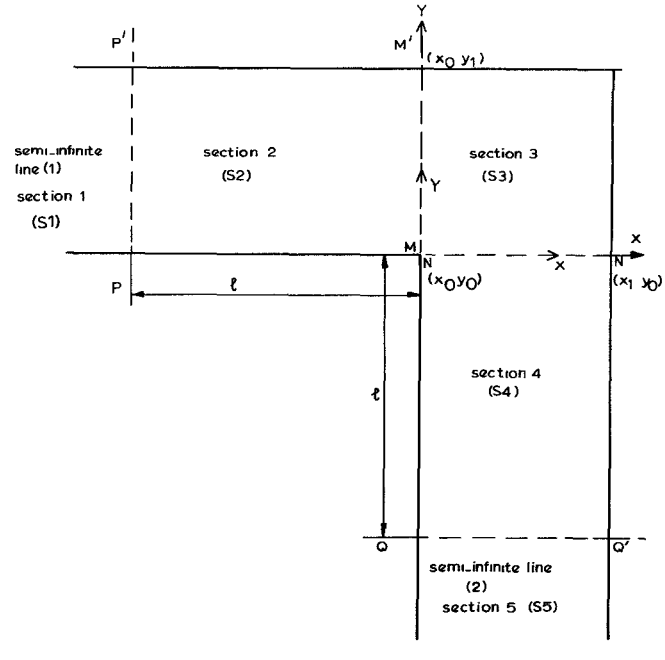

Fig. 1. Plan view of a symmetric right-angle bend in microstrip showing the discontinuity reference planes MM' and NN' and the boundary planes PP' and QQ'. Also shown is the subdivision of the structure in rectangular elements $S1$ to $S5$.

Solving (12) and (11) gives the current distribution in the region bounded by PP' and QQ' in Fig. 1. The total inductance L_T of this region, bounded by PP' and QQ' in Fig. 1, can then be obtained from (8) and (9), and the required discontinuity inductance L_c is obtained by subtracting the inductance of a $2l$ length of equivalent uniform infinite line from L_T. Thus the inductance of the semi-infinite line is assumed to be that of uniform infinite line L_∞, up to the discontinuity reference planes MM' and NN'.

Hence

$$L_c = L_T - 2lL_\infty \tag{13}$$

where

- L_c discontinuity inductance between the reference plane MM' and NN';
- L_∞ inductance per unit length of the uniform infinitely long line;
- L_T total inductance of the section between PP' and QQ';
- l distance of PP' and QQ' from MM' and NN', respectively.

Equation (13) gives L_c from the subtraction of two nearly equal numbers; hence the error in L_c is approximately that of the absolute value of error L_T, hence accuracy of L_c becomes a problem. This is overcome using the excess-current (charge) technique of Silvester and Benedek [10]. The uniform infinite-line current-density distribution $\bar{J}_\infty$ is assumed to exist from $-\infty$ up to MM', and from NN' onwards to $-\infty$; and in the discontinuity MM' to NN' a known current distribution $\bar{J}_d$ is defined to preserve continuity of current. Excess circulating current $\bar{J}_e$ is added in the entire region between PP' and QQ' so that the known assumed current distributions are redistributed to satisfy the governing equation. The magnitude and distribution of this excess circulating current is determined from the solution of (11). The gradient of the impressed potential $\nabla\Phi$ which is the right-hand side (RHS) of this equation can be obtained by the solution of the Laplace's equation on the strip regions between PP' and QQ' with appropriate boundary conditions. Thus (11) becomes

$$\mu_0 \int_{S_1} G_i \bar{J}_{x\infty}\, dS + \mu_0 \int_{S_2} G_i(\bar{J}_{x\infty} + \bar{J}_{e2})\, dS + \mu_0 \int G_i \bar{J}_{e3}\, dS + \mu_0 \int_{S_4} G_i(\bar{J}_{y\infty} + \bar{J}_{e4})\, dS + \mu_0 \int_{S_5} G_i \bar{J}_{y\infty}\, dS = -\nabla\Phi \tag{14}$$

where $\bar{J}_{e3}$ is the sum of $\bar{J}_d$ and $\bar{J}_e$ in this region 3, and $\nabla\Phi$ is known.

Now $\bar{J}_{x\infty}$ and $\bar{J}_{y\infty}$ can be obtained by solving (11) and

(12) for the uniform infinite line with the same w/h values, where w is the width of the strip and h is the thickness of the substrate. Since these currents ($\bar{J}_{x\infty}$ and $\bar{J}_{y\infty}$) vary only with respect to y and x, respectively, the integration with respect to x and y, respectively, can be performed analytically. We also note that $\bar{J}_{x\infty}$ extends from $x = -\infty$ to MM', and $J_{y\infty}$ extends from $y = NN'$ to $-\infty$, thus (14) becomes

$$\mu_0 \int_{S_T} G_i \bar{J}_e \, dS = -\nabla\Phi - \mu_0 \int_{y_0}^{y_1} G_1 \bar{J}_{x\infty} \, dy - \mu_0 \int_{x_0}^{x_1} G_2 \bar{J}_{y\infty} \, d_x \quad (15)$$

where the reference plane MM' is the line $x = x_0$; NN' is the line $y = y_0$; S_T is the strip region between PP' and QQ', and the Green's functions are

$$G_1 = \log_e \left[\frac{(x_0 - x) + \{(x_0 - x)^2 + (y_0 - y)^2 + (2h)^2\}^{1/2}}{(x_0 - x) + \{(x_0 - x)^2 + (y_0 - y)^2\}^{1/2}} \right] \quad (16)$$

and

$$G_2 = \log_e \left[\frac{(y_0 - y) + \{(y_0 - y)^2 + (x_0 - x)^2 + (2h)^2\}^{1/2}}{(y_0 - y) + \{(y_0 - y)^2 + (x_0 - x)^2\}^{1/2}} \right]. \quad (17)$$

Note that these Green's functions are obtained for a semi-infinite line and its image in ground plane. Equation (15) is solved by the Galerkin method, and the solution for $\bar{J}_e$ in each region is used to calculate the excess inductance L_c in the following manner.

From (13)

$$L_c = L_T - 2lL_\infty.$$

Express L_T in terms of $\bar{A}$ and $\bar{J}$ and hence

$$I^2 L_T = \int_{S_T} \bar{A} \cdot \bar{J} \, dS = \int_{S_2} \bar{A} \cdot (\bar{J}_{x\infty} + \bar{J}_{e2}) \, dS + \int_{S_3} \bar{A} \cdot \bar{J}_{e3} \, dS + \int_{S_4} \bar{A} \cdot (\bar{J}_{y\infty} + \bar{J}_{e4}) \, dS. \quad (18)$$

Consider the first term on the RHS of this equation. From (1) we have

$$\bar{A} = \mu_0 \int_{S_1} G_i \bar{J}_{x\infty} \, dS + \mu_0 \int_{S_2} G_i (\bar{J}_{x\infty} + \bar{J}_{e2}) \, dS + \mu_0 \int_{S_3} G_i \bar{J}_{e3} \, dS + \mu_0 \int_{S_4} G_i (\bar{J}_{y\infty} + \bar{J}_{e4}) \, dS + \mu_0 \int_{S_5} G_i \bar{J}_{y\infty} \, dS$$

which simplifies to

$$A = \mu_0 \int_{y_0}^{y_1} G_1 \bar{J}_{x\infty} \, dy + \mu_0 \int_{x_0}^{x_1} G_2 \bar{J}_y \, dx + \mu_0 \int_{S_T} G_i \bar{J}_e \, dS. \quad (19)$$

Hence the first term in (18) becomes

$$\int_{S_2} \bar{A} \cdot \bar{J}_{x\infty} \, dS = \mu_0 \int_{S_2} \int_{y_0}^{y_1} G_1 \bar{J}_{x\infty} \, dy \cdot \bar{J}_{x\infty} \, dS + \mu_0 \int_{S_2} \int_{x_0}^{x_1} G_2 \bar{J}_{y\infty} \, dx \cdot \bar{J}_{x\infty} \, dS + \mu_0 \int_{S_2} \int_{S_T} G_i \bar{J}_e \, dS \cdot \bar{J}_{x\infty} \, dS. \quad (20)$$

Now let

$$I^2 L_{-1/2\infty} = -\mu_0 \int_{S_2} \int_{y_0}^{y_1} G_3 \bar{J}_{x\infty} \, dy \cdot \bar{J}_{x\infty} \, dS$$

where

$$G_3 = \left[\frac{(x - x_0) + \{(x - x_0)^2 + (y_0 - y)^2 + (2h)^2\}^{1/2}}{(x - x_0) + \{(x - x_0)^2 + (y_0 - y)^2\}^{1/2}} \right]$$

and $L_{-1/2\infty}$ is the difference in inductance between a length l m long from the termination point of semi-infinite line and that of a length l m long of infinite line. This term is added to and subtracted from RHS (20): in the addition it combines with first term of (20) to give lL_∞.

Also note that since $\bar{J}_{x\infty}$ and $\bar{J}_{y\infty}$ are perpendicular to each other so that

$$\mu_0 \int_{S_2} \int_{y_0}^{y_1} G_2 \bar{J}_{y\infty} \, dx \cdot \bar{J}_{x\infty} \, dS = 0.$$

Thus

$$\int_{S_2} A \cdot \bar{J}_{x\infty} \, dS = I^2 (lL_\infty - L_{-1/2\infty}) + \mu_0 \int_{S_2} \int_{S_T} G_i \bar{J}_e \, dS \cdot \bar{J}_{x\infty} \, dS. \quad (21)$$

Similarly, simplifications are made for the third term in (18). Thus the whole equation now becomes

$$I^2 L_T = I^2 (lL_\infty - L_{-1/2\infty}) + \mu_0 \int_{S_2} \int_{S_T} G_i \bar{J}_e \, dS \cdot \bar{J}_{x\infty} \, dS + I^2 (lL_\infty - L_{-1/2\infty}) + \mu_0 \int_{S_4} \int_{S_T} G_i \bar{J}_e \, dS \cdot \bar{J}_{y\infty} \, dS + \int_{S_3} \bar{A} \cdot \bar{J}_e \, dS \quad (22)$$

and hence substituting L_T from (22) into (13) gives

$$L_c = L_{\text{CAL}} - 2L_{-1/2\infty} \quad (23)$$

where

$$I^2 L_{\text{CAL}} = \mu_0 \int_{S_2} \int_{S_T} G_i \bar{J}_e \, dS \cdot \bar{J}_{x\infty} \, dS + \mu_0 \int_{S_4} \int_{S_T} G_i \bar{J}_e \, dS \cdot \bar{J}_{y\infty} \, dS + \int_{S_3} \bar{A} \cdot \bar{J}_e \, dS.$$

Although L_c is still obtained by subtracting two values, the numerical error is much smaller since L_c is of the same order as that of L_{CAL} and $L_{-1/2\infty}$

The alternative scheme is to define $\nabla\Phi$ as the sum of two quantities, thus

$$\nabla\Phi = \nabla\Phi_\infty + \nabla\Phi_e \tag{24}$$

where $\nabla\Phi_\infty$ is the gradient obtained in an infinite uniform line and $\nabla\Phi_e$ is the excess gradient due to the discontinuity.

Also from (11) we have

$$\mu_0 \int G_i \bar{J} \, dS = \bar{A} = -\nabla\Phi = -(\nabla\Phi_\infty + \nabla\Phi_e)$$

which is to be substituted in (18). The second term of RHS of (13) becomes

$$2lI^2 L_\infty = -\int_{S_2} \nabla\Phi_{x\infty} \cdot \bar{J}_{x\infty} \, dS - \int_{S_4} \nabla\Phi_{y\infty} \cdot \bar{J}_{y\infty} \, dS. \tag{25}$$

Substituting from (24), (25), and (18) in (13) gives

$$L_c = \frac{1}{I^2}\left[\int_{S_T} \nabla\Phi_e \cdot \bar{J}_e \, dS + \int_{S_T} \nabla\Phi_\infty \cdot \bar{J}_e \, dS + \int_{S_T} \nabla\Phi_e \cdot \bar{J}_\infty \, dS\right]. \tag{26}$$

Note that if the Galerkin method is used with the trial functions for $\bar{J}_e$ being identical to the projection functions, these terms (apart from $\nabla\Phi_e \cdot \bar{J}_\infty$) have all been evaluated in the solution of (15). It would appear on first sight that the latter method would be better since it involves no subtraction. However, it is easily shown that

$$\int \nabla\Phi_e \cdot \bar{J}_\infty \, dS = \mu_0 \int_{S_2} \int_{S_T} G_i \bar{J}_e \, dS \cdot \bar{J}_{x\infty} \, dS + \mu_0 \int_{S_4} \int_{S_T} G_i \bar{J}_e \, dS \cdot \bar{J}_{y\infty} \, dS - 2L_{-1/2\infty} l$$

is often negative, and

$$\int_{S_T} \nabla\Phi_e \cdot \bar{J}_e \, dS + \int_{S_T} \nabla\Phi_\infty \cdot \bar{J}_e \, dS = \int_{S_T} \bar{A} \cdot \bar{J}_e \, dS$$

is most often positive; thus this method also often involves the subtraction of the two numbers. This is also the case in the first method, where the result L_c is obtained as the difference or sum of two numbers.

Also in the latter method the ratio of magnitude of $\nabla\Phi$ to I is important since terms are divided by I^2, and thus any error will appear in the results. However, in the former method, all terms involve the product of two currents, and thus any error in magnitude cancels out. In the former method the term $L_{-1/2\infty}$ is calculated previously using a large number of Gaussian points to obtain the value accurately, whereas in the latter method, $\nabla\Phi$ must be obtained very accurately (0.1 percent) to ensure that term $\int \nabla\Phi_e \cdot \bar{J}_\infty \, dS$ is accurately determined. Thus the method to be used is not clear cut; for the calculations given here the former was used throughout.

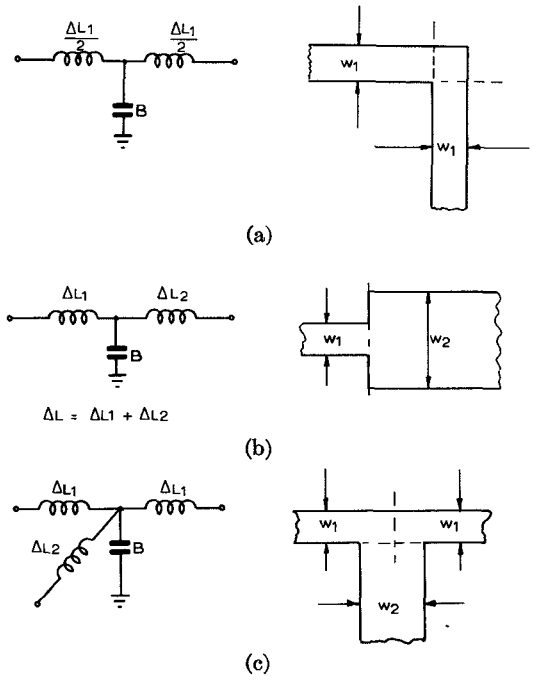

Fig. 2. Equivalent circuits of three microstrip discontinuities with the positions of the reference planes. (a) Symmetric right-angled bend, strip w_1 wide. (b) Step-width change from strip w_1 width to w_2 width. (c) Symmetric T junction, straight arms w_1 wide; vertical, w_2 wide. Substrate thickness kept constant at $h = 1$. The inductances given in these circuits are plotted in Figs. 3–6.

Although the technique is illustrated for a symmetric right-angled corner, the extension to other discontinuities such as the T and step change are simple and require no further elaboration.

The method of numerical implementation is by the Galerkin method and is similar to that used by Gopinath and Silvester [8] and thus will not be included here. The only difference is that the current density $\bar{J}$ requires to be nondivergent, and this is accomplished by defining a vector action potential $\bar{W}$ so that

$$\nabla \times \bar{W} = \bar{J}$$

and hence

$$\nabla \cdot \bar{J} = 0$$

is satisfied.

Since $\bar{J}$ is a two-dimensional vector, J_z being zero, $\bar{W}$ need only have a z-directed component. Thus the preceding equations are recast, replacing $\bar{J}$ by $(\nabla \times W_z)$ and $\bar{J}_e$ by $(\nabla \times W_{ze})$ in the numerical solution. In this case, it was necessary only to ensure continuity of normal component of current or potential $\bar{W}$ at common boundaries between elements. This was implemented using the gen-

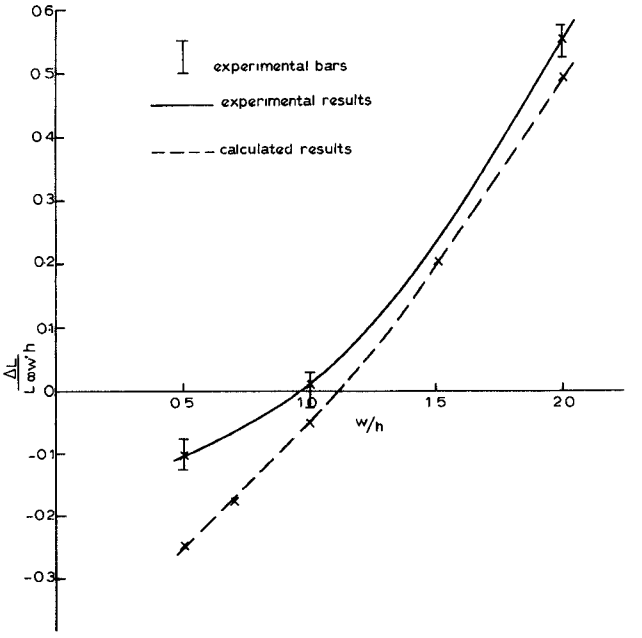

Fig. 3. Normalized inductance of a symmetric right-angled bend $\Delta L/(L_{\infty w}h)$ plotted for different w/h ratios. Comparison is with experimental results from Easter [9].

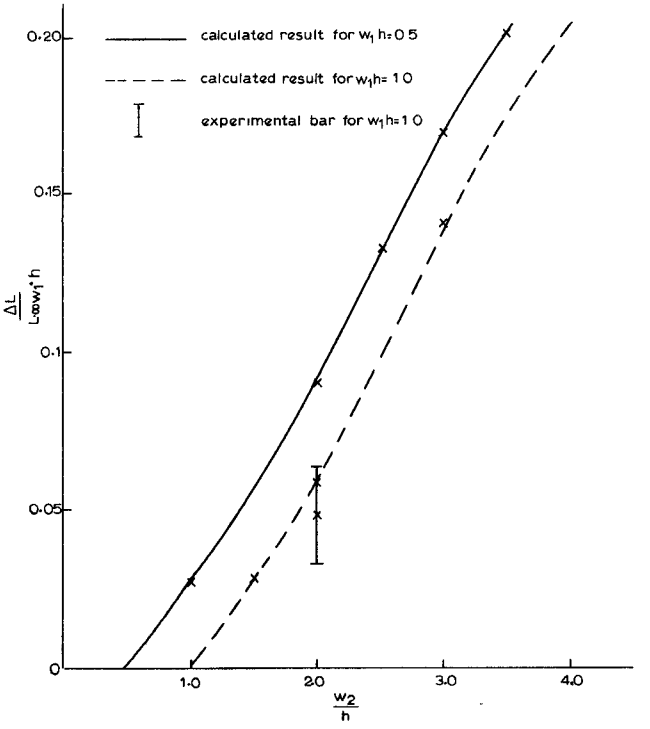

Fig. 4. Normalized inductance for step-width change $\Delta L/(L_{\infty w1}h)$ for $w_1/h = 0.5$ and 1.0 for different w_2/h. Experimental results for one value are marked.

eralized matrix inverse technique also discussed previously [8].

RESULTS AND DISCUSSION

Preliminary tests were performed to check the inductance of straight uniform infinite lines segmented in the center for different w/h values. These results were in excellent agreement with those obtained from Silvester's method of images program [11]. Although this test is essentially trivial, the method and the program operation are checked.

Subsequently, a large number of runs were performed on the step-width change, symmetric right-angled bend, and symmetric T junction, for a number of different w/h. These results compared favorably with experimental results due to Easter [9] as shown in Figs. 2–6. It is apparent

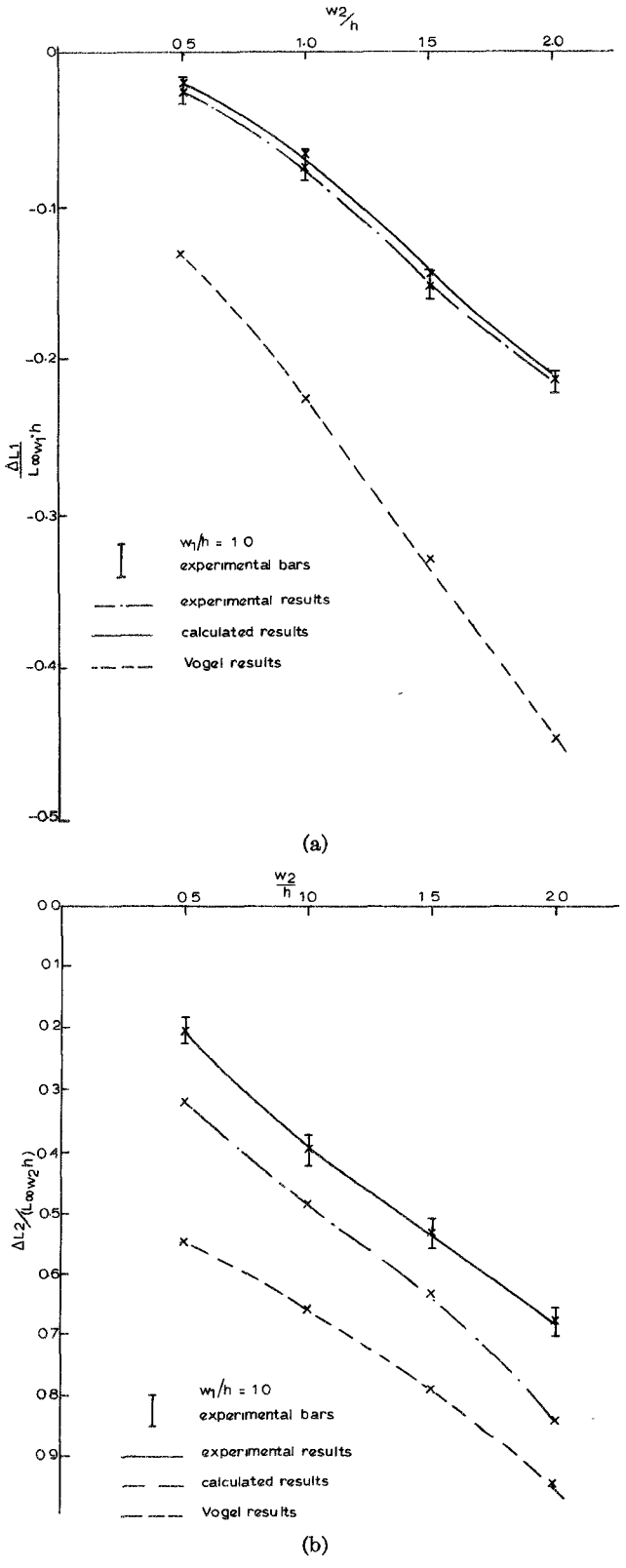

Fig. 5. (a) Normalized inductance of the straight arm of the T junction $\Delta L_1/(L_{\omega w1}h)$ for $w_1/h = 1.0$ for different w_2/h. Comparison is with the experimental results of Easter [9] and calculated due to Vogel [12]. (b) Normalized inductance of the vertical leg of the T, $\Delta L_2/(L_{\omega w2}h)$ for $w_1/h = 1.0$ for different w_2/h. Comparison is with experiment [9] and Vogel [12].

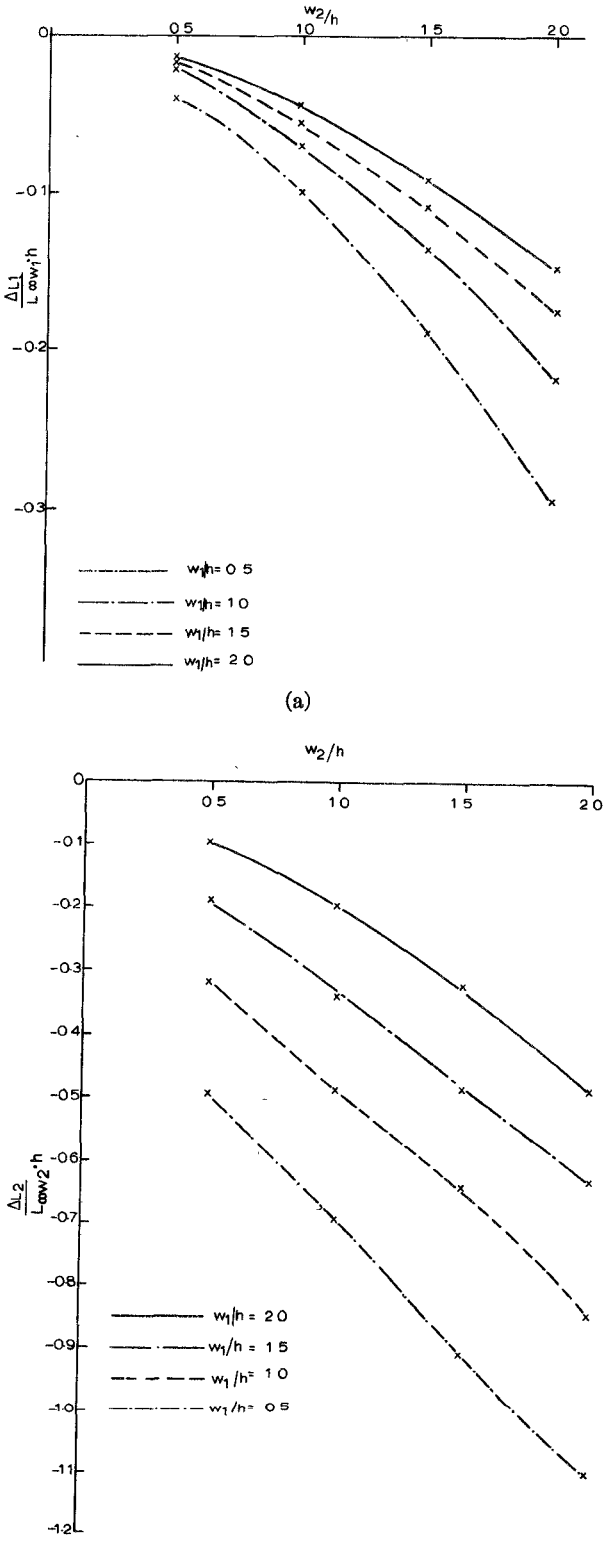

Fig. 6. (a) Normalized inductance of the straight arm of the T, $\Delta L_1/(L_{\omega w1}h)$ for $w_1/h = 0.5$, 1.0, 1.5, and 2.0 for different w_2/h. (b) Normalized inductance of the vertical leg of the T, $\Delta L/(L_{\omega w2}h)$ for $w_1/h = 0.5$, 1.0, 1.5, and 2.0 for different w_2/h.

that the agreement worsens when the experimental inductance values are highly frequency dependent, the estimate falling outside the experimental error range. It is expected that the results for step-width changes and the straight arms of the T are within a few percent of the actual values. For the bend and the vertical leg of the T, the results are somewhat worse and the reason for this are not determined. Fig. 5(a) and (b) shows comparison of

our calculation with those of Vogel [12], and obtains better agreement with the experimental results. Note that experiment shows that these negative line lengths decrease with increasing frequency.

CONCLUSION

A method of calculating quasi-static microstrip discontinuity inductance has been outlined. The computer program written for these calculations has given results which compare favorably with experiment. Curves for some widely used discontinuities have been provided.

ACKNOWLEDGMENT

The authors wish to thank B. Easter for valuable discussions during the course of this work.

REFERENCES

[1] A. Farrar and A. T. Adams, "Computation of lumped microstrip capacitances by matrix methods—Rectangular sections and end effects," *IEEE Trans. Microwave Theory Tech.* (Corresp.), vol. MTT-19, pp. 495–496, May 1971.
[2] ——, "Matrix method for microstrip three-dimensional problems," *IEEE Trans. Microwave Theory Tech.*, vol. MTT-20, pp. 497–504, Aug. 1972.
[3] D. S. James and S. H. Tse, "Microstrip end effects," *Electron. Lett.*, vol. 8, pp. 46–47, 1972.
[4] I. Wolff, "Statischie Kapazitaten von Rechteckigen und Kreisformigen Mikrostrip—Scheibenkondiensatorem," *Arch. Elek. Übertragung.*, vol. 27, pp. 44–47, 1973.
[5] R. Horton, "Electrical characterization of a right-angled bend in microstrip line," *IEEE Trans. Microwave Theory Tech.* (Short Papers), vol. MTT-21, pp. 427–429, June 1973.
[6] ——, "Electrical representation of an abrupt impedance step in microstrip line," *IEEE Trans. Microwave Theory Tech.* (Short Papers), vol. MTT-21, pp. 562–564, Aug. 1973.
[7] A. Gopinath and B. Easter, "Moment method of calculating discontinuity inductance of microstrip right-angled bends," *IEEE Trans. Microwave Theory Tech.* (Short Papers), vol. MTT-22, pp. 880–883, Oct. 1974.
[8] A. Gopinath and P. Silvester, "Calculation of inductance of finite-length strips and its variation with frequency," *IEEE Trans. Microwave Theory Tech.*, vol. MTT-21, pp. 380–386, June 1973.
[9] B. Easter, "An equivalent circuit of some microstrip discontinuities," this issue, pp. 655–660.
[10] P. Silvester and P. Benedek, "Equivalent capacitances of microstrip open circuits," *IEEE Trans. Microwave Theory Tech.*, vol. MTT-20, pp. 511–516, Aug. 1972.
[11] P. Silvester, "TEM wave properties of microstrip transmission lines," *Proc. Inst. Elec. Eng.*, vol. 115, pp. 43–48, Jan. 1968.
[12] R. W. Vogel, "Effects of the T-junction discontinuities on the design of microstrip directional couplers," *IEEE Trans. Microwave Theory Tech.* (Short Papers), vol. MTT-21, pp. 145–146, Mar. 1973.

The Equivalent Circuit of Some Microstrip Discontinuities

BRIAN EASTER

***Abstract*—The experimental characterization of some microstrip structures of common interest, including symmetrical T junctions, is described. Some results are compared with data derived from recent three-dimensional static theory and from the uniform plane-wave model. It is concluded that while the three-dimensional theory requires further improvement, it is generally in much better agreement with the measured data than the two-dimensional uniform plane-wave model.**

I. INTRODUCTION

THERE IS NOW available a substantial body of data on the properties of uniform microstrip lines. In contrast, the circuit designer is often without adequate information on the discontinuity and junction structures comprised in typical practical circuits. Presently available equivalent circuit data fall broadly into two categories. First, there is a growing body of information [1]–[4] on the quasi-static capacitance of microstrip structures, supplemented more recently by studies of the inductance [5]–[7]. In due course this approach should provide accurate quasi-static data on all structures of interest, but, of course, with no indication of dynamic effects. A second source of data derives from the use of a uniform plane-wave parallel plate model of the microstrip cross section as described by Vogel [14] and others, following the method applied by Oliner [8] to symmetrical ("triplate") strip lines: This approach has the great advantage of reducing the problem to two-dimensional complexity. Closed-form expressions are available in classical texts [9] for several quasi-static elements, and some studies [10], [11] have directly tackled the dynamic situation. In addition, reference to Babinet equivalence enables the use of rectangular waveguide data. Against these advantages, there remains the difficulty of any estimation of the error associated with the use of the uniform plane-wave model. It can be noted that not only is the proportion of fringe

Manuscript received November 19, 1974; revised March 27, 1975. This work was carried out as a part of a study supported by the United Kingdom Science Research Council.

The author is with the School of Electronic Engineering Science, University College of North Wales, Bangor, Caerns., LL57 1UT, Wales, U. K.